Dear Phillip,

With the help from one of the native-English-speaker co-authors, the manuscript is now language-edited again thoroughly, including all the minor grammatical issues you've mentioned in a previous round.

About the figures-appeared-twice problem, I checked the uploaded file. The figures now appear only once. I have no idea why previously we encountered an appearing twice problem. In this version, if you still find such a problem in the uploaded file, or there is anything I should do, please let me know.

Thank you for your suggestion and help.

Zhuoyi

The non-conservative distribution pattern of organic matter in the Rajang, a tropical river with peatland in its estuary

Zhuo-Yi Zhu[1]*, Joanne Oakes[2], Bradley Eyre[2], You-You Hao[1], Edwin Sien Aun Sia[3], Shan Jiang[1], Moritz Müller[3], Jing Zhang[1]

1. State Key Laboratory of Estuarine and Coastal Research, East China Normal University, Shanghai, 200241, China

2. Centre for Coastal Biogeochemistry, School of Environment, Science and Engineering, Southern Cross University, Lismore NSW, 2480, Australia

3. Swinburne University of Technology, Faculty of Engineering, Computing and Science, Jalan Simpang Tiga, Kuching, 93350, Sarawak, Malaysia

*Corresponding author: Z.Y. Zhu, zyzhu@sklec.ecnu.edu.cn; zhu.zhuoyi@163.com

Abstract

South-east Asian peatland-draining rivers have attracted much attention due to their high dissolved organic carbon (DOC) yield and high CO_2 emissions under anthropogenic activities. In August 2016, we carried out a field investigation of the Rajang river and estuary, a tropical system located in Sarawak, Malaysia. The Rajang has peatland in its estuary, while the river basin is covered by tropical rainforest. DOC $\delta^{13}C$ in the Rajang ranged from -28.7‰ to -20.1‰ ~~and~~, with a U-shaped trend from river to estuary ~~was identified.~~. For particulate organic carbon (POC), ~~the~~ $\delta^{13}C$ ranged between –29.4‰ ~~to~~and –31.1‰ in the river and there was a clear increasing trend towards more ~~$\delta^{13}C$~~ enriched $\delta^{13}C$ values with higher salinity ~~existed in the estuary~~. In the estuary, there was a linear conservative dilution pattern for dissolved organic matter composition (as quantified by D/L amino ~~acids~~acid enantiomers) plotted against DOC $\delta^{13}C$, whereas when plotted against salinity dissolved D/L amino ~~acids~~acid enantiomers values were higher than the theoretical dilution value. Together, these data indicate that the addition of DOC ~~in~~to the estuary (by peatland) not only increased the DOC concentration, but also altered its composition, by adding more bio-degraded, ^{13}C-depleted organic matter into the bulk dissolved organic matter. Alteration of organic matter composition (~~adding~~addition of a more degraded subpart) was also apparent for the particulate phase, but patterns were less clear. The Rajang was characterized by DOC~~/DON~~ to DON (dissolved organic nitrogen) ratios of 50 in the river section, with loss of DON in the estuary ~~increased~~increasing the ratio to 140, suggesting ~~the~~ unbalanced export ~~pattern for~~of organic carbon and nitrogen~~, respectively~~.. Under anthropogenic activities, further assessment of organic carbon to nitrogen ~~ratio~~ratios is needed.

Keyword

Amino ~~acids~~acid enantiomers, DOC, POC, stable carbon isotope, Rajang, peatland

1. Introduction

Fluxes and cycling of organic matter (OM) in rivers and estuaries are important influences on global biogeochemical cycles and climate change. In river basins, vascular plants are the ultimate sources of organic matter (Hedges and Man, 1979), but algae, moss, and bacteria are also important (Hernes et al., 2007). As well as providing a source of OM, bacteria may ~~also~~ strongly modify the composition of organic matter within a river and its resistance to degradation. The lability of organic matter determines how rapidly organic carbon will be transformed into inorganic carbon (CO_2), which can vary from hours to millions of years. The lability of organic matter therefore plays a role in determining whether organic matter is either a source or a sink of carbon in the atmosphere (Zhang et al., 2018). Based on ^{14}C ~~of~~in organic carbon, Mayorga et al. (2005) determined that the degradation of recently synthesized organic matter in the river basin was the main reason Amazonian river waters were supersaturated in CO_2, and hence ~~the~~ a source of atmospheric CO_2. This highlights the potential importance of organic matter stability for carbon cycling within river systems. Nitrogen is another important element in organic matter, which is not independent ~~from~~of carbon, but instead is closely combined with carbon in various chemical compounds (like amino acids). Due to the nature of these specific compounds, the behavior of bulk carbon and nitrogen can differ substantially. In basins with peatland, the leaching of DOC is related to the status of peatland (disturbed vs undisturbed), whereas the leaching of dissolved organic nitrogen (DON) is controlled by the soil inorganic nitrogen content (Kalbitz and Geyer, 2002). The different leaching mechanisms of organic carbon and nitrogen indicates that the comparison of these two elements would deepen our understanding of organic matter cycles.

Tropical south-east Asian rivers play an important role in both dissolved and particulate organic

matter export (Baum et al., 2007; Huang et al., 2017; Müller et al., 2016). Located in Sarawak, Malaysia (Fig. 1a), the turbid Rajang river (hereafter refer to as the Rajang) is the longest river in Malaysia. The Rajang flows through tropical rainforest, and peatland and mangroves are distributed in the estuary. A dam was constructed in the upper reaches of the Rajang in 2015, but the total suspended matter (TSM) in the river remains at 100 – 200 mg/L ~~in recent years~~ (Müller-Dum et al., 2019). ~~Dilution of~~This terrestrial organic matter ~~in~~can be expected to be diluted at the adjacent coast ~~is expected, while turbid~~, given that the turbidity of the river ~~water~~ strongly limits ~~apparent~~ organic matter photo-degradation within the river and estuary~~, leaving the stage of fluvial~~. Fluvial organic matter ~~alteration to bacteria~~is therefore dominated by bacterial utilization and abiotic ~~process like~~processes such as desorption/adsorption between particulate and dissolved ~~phase~~phases (Martin et al., 2018). Further, dissolved oxygen is negatively related to pCO_2, likely due to in-stream heterotrophic respiration (Müller-Dum et al., 2019). In the Rajang brackish estuary, where peatland is located, addition of peatland DOC into river water is suggested by the non-conservative mixing pattern of DOC with increasing salinity (Martin et al., 2018), whereas removal of DON in the Rajang estuary is suggested by nitrogen stable isotopes (Jiang et al., 2019).

While stable isotopes of carbon and nitrogen are useful tools for tracing organic matter, amino acids (AAs) are the most important organic carbon and nitrogen carriers that have been chemically identified, accounting for up to ~100% of the particulate nitrogen in aquatic environments, and up to nearly half of the particulate organic carbon pool (Jennerjahn et al., 2004). Due to the selective removal and accumulation of certain amino acids, amino acids are important biomarkers in early diagenesis, allowing quantification of organic matter lability/resistance (Dauwe and Middelburg, 1998; Kaiser and Benner, 2009). With the exception of glycine, amino acids are chiral. L forms of

amino acids are from animals, plants and plankton, whereas D forms mainly come from bacteria, and are key chemical compounds in peptidoglycan, which forms the basic structure of bacterial cell membranes (Vollmer et al., 2008). Due to the key role of bacteria in OM alteration and early diagenesis, D-AAs (D forms of AAs) tend to accumulate during OM degradation. A higher ratio of D- to L-AAs (D/L ratio) therefore indicates ~~more~~ that OM is more refractory (Davis et al., 2009). As a non-protein amino acid, accumulation of GABA (γ－aminobutyric acid) is also highly related to OM degradation (Davis et al., 2009). Conversely, a lower D/L ratio and GABA% indicates that OM is relatively less degraded, and hence more labile. In river waters, elevated D-AAs also ~~indicates~~indicate the presence of soil humic substances, which ~~is~~are a product of bacteria and their detritus (Kimber et al., 1990).

Tropical rivers are dominated by refractory (or bio-degraded) organic matter, yet labile OM is also known to play a role in river carbon cycles (Mayorga et al., 2005). It is hence expected that ~~the~~ fluvial organic matter ~~in the~~within a river would be a mixture of labile organic matter (~~that~~which can be respired to support pCO_2) and refractory terrestrial organic matter (~~that~~which will be diluted/degraded after entering the sea (Martin et al., 2018)~~,~~), while in the estuary there would be addition of dissolved OM from peatland/mangrove (Dittmar et al., 2001b; Müller et al., 2016). Previous studies of OM in south-east Asian rivers mainly focused on its bulk concentrations, ages, or optical properties (Martin et al., 2018 and ref. therein). The use of biomarker approaches has been very limited (Baum et al., 2007; Gandois et al., 2014). Given the processes described above and their potential contribution to the carbon (Müller-Dum et al., 2019) and nitrogen cycles (Jiang et al., 2019), it is somewhat surprising that there has been limited application of amino acid approaches, including D-AAs, to investigate organic matter composition and the role of estuarine

peatland/mangrove in OM regulation (Jennerjahn et al., 2004). South-east Asian rivers are subject to multiple stressors due to increasing anthropogenic activities in both their riverine (e.g., damming, logging/secondary plantation) and estuarine sections (e.g., drainage, and oil palm plantations) (Hooijer et al., 2015). ~~AAs~~Amino acid enantiomers and carbon/nitrogen isotopes have the ability to provide molecular level evidence for the impact of these stressors on carbon and nitrogen cycling and bulk biogeochemistry, as well as insight into the mechanisms underlying such changes.

In this study, we carried out a field investigation in the Rajang in August 2016, from stations S10 to S1~~ station~~, located on the coast of the South China Sea adjacent to the Rajang (Fig. 1b). ~~AAs~~AA enantiomers and $\delta^{13}C$ values of DOC were used to elucidate the succession of organic matter sources/composition from the fresh water to the estuarine sections of the Rajang. Our aim was to address the following questions: 1) Given that peatland contributes additional DOC to fluvial DOC (Müller et al., 2016), does the composition of dissolved OM change from river to estuary? 2) Do changes in organic nitrogen mirror changes in organic carbon? 3) ~~And hence~~Hence, what is the role of peatland/mangroves on OM composition and lability in the Rajang? Globally, rivers ~~in~~at low latitudes receive much less attention relative to temperate and polar rivers (36 vs. 958 studies~~)~~) (Cloern et al., 2014), while they could be equally important ~~in~~for global carbon ~~cycle~~cycles (Cloern et al., 2014). ~~Our work, together with other tropical studies, would enrich the understandings for~~This study ultimately aims to enrich our understanding of organic carbon and nitrogen cycles in tropical rivers/estuaries.

2. Materials and methods

All abbreviations, together with the amino acids measured in this study, are listed in table 1.

2.1 Brief background

The Rajang river and estuary is located in Sarawak, Malaysia. The climate is wet year-round, but the main precipitation typically occurs in winter (November to February). Climate is influenced by the El Niño-Southern Oscillation (ENSO) and Madden-Julian Oscillation. In August 2016, the discharge was estimated as 2440 m^3/s, in comparison with an annual mean discharge of 4000 m^3/s for 2016 and 2017 (Müller-Dum et al., 2019).

Based on salinity, station S5 is regarded as the boundary of the fresh and estuarine water of the Rajang (Fig. 1b). In this work all samples with a salinity of 0 were regarded as fresh water, while samples with salinity >0 were regarded as estuarine. In the estuary, there are several branches, namely Igan, Lassa, Paloh, and Rajang itself (Fig. 1b). Since water in all these branches ~~are~~is derived from the Rajang river (i.e., upstream of S5), in this ~~work~~study all these branches are regarded as the Rajang estuary. Peatland and mangroves are ~~commonly distributed~~common in the estuary (shown in Fig. 1b) while tropical rainforest is widely distributed upstream of S5 (not shown in Fig. 1b). The peatland is under strong pressure of draining and change of use for oil palm plantations, while ~~in the basin~~ logging and secondary growth is very common in the river basin (Hooijer et al., 2015). Compared with other peatland-draining tropical blackwater rivers, the Rajang is more like a turbid tropical rainforest river (Müller-Dum et al., 2019), but with notable peatland/mangrove in its estuary (Fig. 1b).

2.2 Field sampling

The field work was carried out in August 2016. The sampling stations covered from S10 (the upper most station in this study) to S1 on the coast. At each station, a pre-cleaned and sample-rinsed bucket was used to collect surface water from the center of the channel in a boat. After sample

collection, pretreatment was done immediately on board ~~in~~ the boat. For DOC and its stable carbon isotope ratios ($\delta^{13}C$), water samples were collected by syringe filtering (pre-combusted Whatman GF/F; 0.7 µm) approximately 30 ml of sample water into a pre-combusted 40 ml borosilicate vial. Samples were preserved with five drops of concentrated phosphoric acid and sealed with a lid containing a Teflon-coated septa. For total dissolved amino acids (TDAA), water samples were filtered through a 0.4 µm nylon filter. For particulate OM samples (TSM, POC, POC-$\delta^{13}C$, PN and PN-$\delta^{15}N$, and total particulate amino acids (TPAA)), suspended particles were concentrated onto glass fiber ~~membrane~~filters (pre-combusted Whatman GF/F; 0.7 µm). The GF/F filters were folded and packed in pre-combusted aluminum. All samples were immediately stored frozen (–20°C) until analysis. At every station both particulate and dissolved samples were collected, but a few samples were lost (broken~~/missing~~) during transportation back to Shanghai. ~~This includes~~The lost samples were the particulate samples (POC and TSM) ~~samples at station~~from stations S16 (conductivity = 64 µS/cm), ~~station~~ S4 (salinity = 4.8), ~~station~~ S25 (salinity = 11.7) and ~~at station~~ S29 (salinity = 4.3~~)~~), and a total dissolved AA sample (TDAA) ~~sample at~~from station S24 (salinity = 19.1). A portable meter (Aquaread, AP-2000) was used to obtain conductivity/salinity, temperature, dissolved oxygen and pH.

2.3 Laboratory analyses

Concentrations and $\delta^{13}C$ of DOC were measured at the Centre for Coastal Biogeochemistry at Southern Cross University (Lismore, Australia) via continuous-flow wet oxidation isotope-ratio mass spectrometry using an Aurora 1030W total organic carbon analyzer coupled to a Thermo Delta V Plus IRMS (Oakes et al. 2010). Glucose of known isotopic composition dissolved in He-purged Milli-Q was used as a standard to correct for drift and to verify sample concentrations and $\delta^{13}C$

values. Reproducibility for concentrations and $\delta^{13}C$ was ± 0.2 mg l^{-1} and ± 0.4 ‰. ~~DOC concentrations and $\delta^{13}C$ were measured at the Centre for Coastal Biogeochemistry at Southern Cross University (Lismore, Australia).~~ For the determination of POC, samples (GF/F glass fiber ~~filter~~filters) were freeze-dried and analyzed with a CHNOS analyzer (Model: Vario EL III) after removing the inorganic carbon by reaction with HCl vapor. For PN, a similar procedure ~~like that of POC~~ was ~~used, but~~followed, with no acid ~~was used in pre~~ treatment. The detection limit for POC was 7.5×10^{-6} g, with precision better than 6%, based on repeated determinations (Zhu et al., 2006). The POC-$\delta^{13}C$ and PN-$\delta^{15}N$ values were determined using a $DELTA^{plus}$/XL isotopic ratio mass spectrometer (Finnigan MAT Com. USA) interfaced with a Carlo Erba 2500 elemental analyzer. The standard for $\delta^{13}C$ was PDB and the precision of the analysis was ± 0.2‰. For $\delta^{15}N$, the standard was air and precision was ± 0.3‰.

Total hydrolyzable AAs were extracted and analyzed following the method of Fitznar et al., (1999) with slight modifications (Zhu et al., 2014). Briefly, samples were first hydrolyzed with HCl at 110°C. After pre-column derivatization with o-Phthaldialdehyde (OPA) and N-Isobutyryl-L/D-cysteine (IBLC/IBDC), AAs and their enantiomers were analyzed using an HPLC (Agilent 1200) comprising of an online vacuum degasser, a quaternary pump, an auto-sampler, a thermostatted column and a fluorescence detector (excitation 330 nm, emission 445 nm). The analytical column was a Phenomenex Hyperclone column (BDS C18, 250×4mm, 5µm) with a corresponding pre-column. To eliminate the influence of racemization of L-type AAs in the hydrolysis process, the concentration of D/L-AAs measured in actual samples was corrected according to the formula obtained by Kaiser and Benner (2005). The detection ~~limit~~limits for glycine (Gly) and individual AAs enantiomers were in the lower picomolar level. Asx and Glx were used for aspartic acid +

asparagine and glutamic acid + glutamine, respectively (Table 1), as the corresponding acids are formed via deamination during hydrolysis.

A few samples (e.g., TDAA in S1 station) were not measured due to instrument hardware ~~problem. And hence the measured~~problems. Therefore, there is not always corresponding particulate and dissolved ~~sample~~data for some stations ~~did not exactly match.~~ .

3. Results

In August 2016, the TSM concentration in the Rajang ranged from 22 mg/L ~~(mean for~~to 161 mg/L. Mean TSM concentrations in the fresh water ~~section: 61 mg/L) to 161 mg/L (mean for the~~and estuarine ~~section: 73~~sections were 61 mg/L and 161 mg/L~~)~~, respectively (Table 2). Throughout the system DOC concentrations exceeded POC concentrations. DOC and POC in the fresh water section averaged 337 μM and 86 μM, and in the estuarine section 345 μM and 64 μM, respectively (Table 2). ~~While~~ DOC ~~concentration was~~concentrations were slightly higher in the estuary than in the fresh water section (Table 2), ~~a~~and maximum ~~of~~concentrations for both DOC and POC ~~can be~~were found at around salinity 15 to 20 in the estuary (Fig. 2).

DOC $\delta^{13}C$ ranged from –28.7‰ to –20.1‰ (Table 2). There was A U-shaped trend in DOC $\delta^{13}C$ from the fresh water ~~section~~ to the estuary section can be identified for ~~DOC $\delta^{13}C$~~, with one outlier from the Rajang main stream at a salinity of 5 (S2 station; Fig. 3a). The minimum ~~value of~~ DOC $\delta^{13}C$ (bottom of the U) was detected at a salinity of ~10 (Fig. 3a). For particulate OM, $\delta^{13}C$ ranged between –29.4‰ to –31.1‰ in the fresh water section. In the estuary section, there was a clear increasing trend with increasing salinity, from –30‰ (S=1.1) to values close to –24‰ (S>30) (Fig. 3b).

In the fresh water section, the mean TDAA and TPAA concentrations were 0.3 μM and 2.5 μM, respectively (Table 3). For TDAA, the AA carbon yield (the carbon from AA divided by bulk DOC or POC, in %) was similar in both fresh water and estuary sections ~~were very similar~~, namely 0.40% and 0.38% (mean), respectively (Table 3~~), whereas~~). In contrast, AA nitrogen yield was higher in the estuary (11%) than in the fresh water section (4.8%) (Table 3). For TPAA, there was little difference between the fresh water and estuary sections in AA carbon yield (13.5% and 16.8%, respectively) and nitrogen yield (66% and 62%, respectively) (Table 3).

~~With respect to individual AA compounds, in~~In the both dissolved and particulate phase, Gly, Glx, Ala and Asx were the most abundant ~~AAs~~AA compounds. These four AAs together accounted for 66% of TDAA and 47% of TPAA in the fresh water section, and 59% of TDAA and 48% of TPAA in the estuary. The non-protein AA GABA was detected in trace amounts, but was ~~accumulated~~more abundant in the dissolved phase ~~relative to~~than in the particulate phase, as indicated by the higher GABA% in the dissolved phase (Table 3). GABA% decreased from 2% (fresh water section mean) to 1.3% (estuarine section mean) in the dissolved phase, and decreased from 0.7% (fresh water section mean) to 0.4% (estuarine section mean) in the particulate phase (Table 3). In the estuary, GABA% in the dissolved phase remained stable (~1.5%) in brackish water (salinity 5 to 20) and quickly dropped to <1% where salinity was over 30 (Fig. 4a). Most of the GABA% ~~data dots were~~values lay above the theoretical mixing line (Fig. 4a). In the particulate phase, there was an overall decrease in GABA% with increasing salinity within the estuary (Fig. 4b).

~~As for the AA enantiomers, the~~ The percentage of D- form ~~AA~~enantiomers of AAs in TDAA averaged 12% for both fresh water and estuarine ~~section. The~~ sections, with Glx and Asx being the

most abundant D- form AAs ~~in the dissolved phase were Glx and Asx. For the particulate phase,~~ The percentage of D- form ~~AA in TPAA~~AAs was much lower ~~relative to that in dissolved form~~in TPAA, decreasing from a mean of 4.4% in the fresh water section to a mean of 3.3% in the estuary (Table 3). ~~And patterns~~Patterns in the variation of D/L Glx (Fig. 5) along ~~with~~the conductivity/salinity gradient in the Rajang were similar to those for GABA% (Fig. 4) for both dissolved and particulate ~~phase. For example, for dissolved phase, the pattern of decreasing D/L ratio along with increasing salinity was nearly absent (Fig. 5a), whereas for particulate phase such decreasing pattern was much clearer in the estuary (Fig. 5b).~~phases. Similar to GABA%, all the dissolved samples ~~showed~~in the estuary had elevated values for D/L Glx (i.e., ~~dots~~values above the theoretical dilution line) ~~for D/L Glx in the estuary~~ (Figs. 4a and 5a).

4. Discussion

4.1 Distribution patterns of OM composition

Dissolved OM

Terrestrial OM usually has a more negative $\delta^{13}C$ value (–32‰ to –26‰ for C3 plants), whereas marine OM has more positive ~~value~~ values ($\delta^{13}C$, ~ –20‰~~)~~) (Lamb et al., 2006; Mayorga et al., 2005). Overall, the very negative $\delta^{13}C$ values for DOC (<–26‰) in the ~~river part~~riverine section of the Rajang ~~indicates~~clearly indicate that the OM had a ~~very clear~~ C3 plant source (e.g., mangroves and oil palms (Jennerjahn et al., 2004; Lamade et al., 2009; Wu et al., 2019)), whereas DOC $\delta^{13}C$ values > –24‰ in the estuary (salinity >30) ~~suggests~~suggest a mixture of terrestrial and marine OM sources (Fig. 3a). The most depleted $\delta^{13}C$ values for DOC occurred at a salinity of 10 (Fig. 3a). Above this salinity, the influence of marine OM became more overwhelming, and the bulk DOC

258 $\delta^{13}C$ signal was more enriched (Fig. 3a).

259 Among samples in the fresh water section, the ~~sample of~~ most enriched DOC-$\delta^{13}C$ ~~value~~values
260 (S10 and S15; DOC-$\delta^{13}C$: –25‰; Fig. 3a~~)~~), although initially appearing to be outliers, were
261 characterized by very elevated D/L amino acids ratios (Fig. 6a). This was particularly the case for
262 the sample from S10 (the upper most station in this study; Fig. 1b), which showed a maximum D/L
263 Glx ratio of 0.57 (Fig. 6a). In addition, these samples from S10 and S15 also showed a higher D/L
264 ratio for Asp (S10: 0.49, S15: 0.38; figure not shown) when compared to all fresh water or estuary
265 samples (mean: 0.34; Table 3). On land, D- form amino acids can be derived from abiotic
266 racemization. This process ~~(which requires~~occurs over a very long time scale~~)~~ (e.g., over thousands
267 of years) and results in ~~which~~ L- form amino acids slowly ~~changes~~changing into their corresponding
268 D- form (Schroeder and Bada, 1976). More significantly, in contemporary environments~~,~~ D- form
269 amino acids are widely synthesized by bacteria during ~~their~~ cell membrane construction (Schleifer
270 and Kandler, 1972). D/L Glutamic acid and D/L Aspartic acid ratios of pure peptidoglycan
271 (*Staphylococcus aureus*, Gram-positive) are 0.49 and 0.30, respectively (Amon et al., 2001).
272 ~~Though~~Although $\delta^{13}C$ values for bacteria in the Rajang ~~remains unclear~~remain unknown, bacteria
273 have been reported to have $\delta^{13}C$ values from –12‰ to –27‰ (Lamb et al., 2006). Contribution of
274 OM derived from bacteria may therefore explain the relatively enriched $\delta^{13}C$ values observed at
275 inland ~~S10~~ station S10 and station S15. A possible OM source at these stations is soil humic
276 substances, which ~~is~~are expected to ~~be under strong impact of bacteria, and has~~have a high
277 contribution ~~of~~from bacteria, and therefore D-form amino acids (Dittmar et al., 2001a). A more
278 depleted pattern of DOC $\delta^{13}C$ from mountain to lowland is suggested to be due to dilution and
279 mixing with younger OM in the lowland (Mayorga et al., 2005). This is consistent with ~~our findings~~

~~that, depleted~~ the pattern we observed of ~~riverine~~depleted DOC $\delta^{13}C$ values within the fresh water section ~~was~~ corresponding ~~to a lowering~~with lower D/L ~~ratio~~ratios pattern, which ~~indicates the~~suggests dilution with less degraded OM (see orange circles in Fig. 6a). Whether the ~~dissolved samples with~~ elevated D/L ~~ratio~~ratios and relatively positive $\delta^{13}C$ values for dissolved samples in the fresh water section ~~(~~at S10 and S15~~;~~ (Fig. 6a) reflect the presence of soil humic substances, or instead reflect the direct presence of bacteria, requires further study.

In the estuarine section, it was very clear that terrestrial bio-degraded OM (indicated by elevated D/L ratios and more negative $\delta^{13}C$) is diluted with more labile OM (lower in D/L ratio but more positive $\delta^{13}C$~~)~~) (see ~~blue~~ solid ~~dots~~blue data points in Fig. 6a). However, this apparent dilution trend became ~~very vague (~~less clear or showed no trend) when D/L ratio was plotted against salinity (Fig. 5a). This was also confirmed by the GABA% distribution pattern which showed a platform-like pattern at a salinity between 5 and 20 (Fig. 4a). Though TDAA at S1 ~~is~~was missing, the composition of TDAA at S2 (salinity = 31.2) was very typical of marine OM (i.e., very low D/L ratio and relatively enriched DOC-$\delta^{13}C$; ~~see~~ Fig. 6a). Hence ~~in the estuary~~ there is a conservative distribution pattern for dissolved OM in the estuary when plotted against $\delta^{13}C$ (Fig. 6a) but ~~such pattern disappeared~~not when plotted against salinity (Figs. 4a&5a). The location above the conservative dilution line of all OM data in the brackish estuary (salinity ~~between~~ 10 ~~and~~to 25; Figs. 4a~~&~~ & 5a), indicates that the OM in the estuarine section was more degraded than theoretically expected. The combination of degraded OM ~~with the observed~~and DOC concentration increase in the estuary (345 μM in the estuary vs. 337 μM in the fresh water section; ~~or~~ Fig. 2b), suggests the addition of degraded DOC to the Rajang. Non-conservative dissolved OM behavior in the estuary has previously been reported based on an optical approach (Martin et al., 2018), and minimal OM

alteration during estuarine transport was suggested (Martin et al., 2018). Hence, it is ~~reasonable~~likely that changes in dissolved OM composition (Figs. 4a~~&~~ & 5a) may largely take place in land/estuary (e.g., in pore waters of soil) and impact the Rajang riverine dissolved OM via leaching from soils.

Particulate OM

~~As for particulate OM~~In the river section of the Rajang, depleted POC-$\delta^{13}C$ ~~in the river part of the Rajang~~ indicated the strong influence of terrestrial OM ~~(e.g., C3 plant; Dittmar et al., 2001b) whereas in the estuary, particulate OM~~ ; this OM is likely derived from C3 plant material, which is a major component of the sediment OM (Wu et al., 2019). In the estuarine section of the Rajang, there was seaward enrichment of POC-$\delta^{13}C$ (Fig. 3b), suggesting that the OM was diluted with marine particulate OM, ~~as indicated by the seawards enrichment of $\delta^{13}C$ (Fig. 3b). In the sediment, a clear woody angiosperm C3 plants as the OM source is found based on a lignin approach (Wu et al., 2019),~~ and aligning with similar ~~increases in carbon and nitrogen isotopes in~~isotope enrichment of suspended particles in brackish water ~~have also been~~ observed in other estuaries (Cifuentes et al., 1996; Raymond and Bauer, 2001). Unlike dissolved OM, there were no POC samples with unusually enriched $\delta^{13}C$ values in the fresh water section (Figs. 6b&c). D/L Glx ~~ratio~~ ratios of particulate OM in the fresh water section ~~is~~was higher when compared with that in the estuary section (Table 3), and overall, when compared with dissolved OM, particulate OM basically became more labile when ~~transporting~~transported seawards, as indicated by shifts in its composition ~~shift along~~ (Figs. 4b&5b) and isotope ratio with salinity (Figs. ~~4b&5b) or isotope (Figs.~~ 6b&c).

Although particulate OM had a lower D/L ratio than dissolved OM (Fig. 6), it should be noted that this does not imply that mean dissolved OM is more aged or degraded than particulate OM.

带格式的
带格式的
带格式的
带格式的
带格式的
带格式的
带格式的
带格式的

Riverine POM and DOM usually show different ages (Bianchi and Bauer, 2011), ~~while~~and this can be influenced by selective desorption/adsorption of bacteria and related detritus between the particulate and dissolved ~~phase also~~phases which can strongly ~~modifies~~modify the biomarker-indicated degradation status of OM (Dittmar et al., 2001a).

4.2 Different fate of bulk organic carbon and nitrogen

Leaching of DOC and DON from peatlands is driven by ~~difference~~different mechanisms: DOC release is related to the status of peatland (pristine vs. degraded), whereas DON release is determined by the DIN content of peatland soil (Kalbitz and Geyer, 2002). In the Rajang, bulk DOC and DON concentrations were not coupled, as ~~suggested~~indicated by ~~the~~variations in DOC/DON ~~ratio variation pattern~~ratios (Fig. 7). The average DOC concentration in the estuary part was slightly higher (345 μM) than in the river part (337 μM; Table 3), ~~which indicates~~suggesting the addition of DOC in the estuary. In comparison, ~~the~~there appears to have been removal of DON in the estuary ~~is suggested~~ (Jiang et al., 2019).

In the Rajang, estuarine DOC exhibited non-conservative dilution behavior ~~from~~based on optical properties ~~was observed for estuarine DOC~~ (Martin et al., 2018), which is consistent with other peatland-draining rivers in Sarawak (Müller et al., 2016). The contribution of marine sources to dissolved OM is reflected in the increasing DOC-$\delta^{13}C$ in the estuary part (Fig. 3a). Peatland, however, is known for its high contribution to fluvial DOC and has been suggested to contribute to the DOC in the Rajang (Martin et al., 2018). In peatland-draining rivers west of the Rajang, the DOC concentration endmember can be as high as 3690 μM (Müller et al., 2015)~~.~~(Müller et al., 2015). Under such high DOC background, a simple three-~~endmember~~point mixing model ~~(i.e., a model that based on the~~, with endmembers of ~~first~~(1) observed ~~fresh water~~fluvial DOC ~~endmember,~~

~~second~~concentration, (2) peatland DOC ~~endmember~~concentration, and ~~third a calculated fresh water~~(3) inferred fluvial DOC ~~endmember)~~concentration from a marine-river mixing curve, suggested that peatland-DOC addition accounts for 3% of the fluvial DOC in the Saribas ~~river~~River and 15% in the Lupar ~~river~~River (Müller et al., 2016). Assuming that peatland in the Rajang estuary has a comparable endmember DOC concentration to other peatland in Sarawak (i.e., 3690 μM; Müller et al., 2015), and given our observed Rajang fresh water DOC endmember value of 337 μM (DOC concentration at S5 station) and a marine DOC endmember of 238 μM (S1 station), a similar mixing model approach suggests that peatland DOC ~~addition~~ contributed 4% of the Rajang fluvial DOC, which is comparable to the Saribas ~~river~~River and much lower than the Lupar ~~river~~River (Müller et al., 2016). In the meantime, as mentioned in the previous section, there is a non-conservative dilution pattern, with dissolved OM in the estuary part more degraded than expected based on simple dilution with a marine endmember (Figs. 4a~~&~~ & 5a). Hence it is reasonable that peatland not only contributed to the fluvial DOC in concentration (Martin et al., 2018), but also modified the dissolved OM composition (more bio-degraded) in the estuary. In another tropical river study, ~~mangrove~~mangroves in the estuary exerted a stronger influence on fluvial dissolved OM than hinterland vegetation (Dittmar et al., 2001b). This is consistent with the Rajang, for which estuarine processes apparently impact the dissolved OM in terms of both DOC concentration (by increasing the bulk amount) and composition (by adding bio-degraded DOC). The estuarine dissolved OM showed higher bio-degraded ~~feature~~characteristics (e.g., elevated GABA% and D/L ratio; Figs. 4a&5a), but this subpart may be photolabile (Martin et al., 2018). ~~When~~Photodegradation is expected to be enhanced when TSM decreases and light ~~condition~~penetration in the water column ~~becomes good~~increases (e.g., ~~entering~~as OM enters the

sea~~), photodegradation is expected~~) (Martin et al., 2018). Other oceanic degradation mechanisms include the priming effect (Bianchi, 2011). The fate of the terrestrial OM in the sea requires further study. As we lack the DON concentration endmember in peatland, peatland impact on DON in the estuary ~~is~~was not estimated in the current study.

In contrast to DOC, which was apparently added to the estuary, DON was removed, contributing to a remarkable increase of dissolved inorganic nitrogen in the estuary (Jiang et al., 2019). In the fresh water section, the nitrate concentration was not related to the ratio of D/L dissolved AAs, nor ~~related to~~ dissolved GABA% (Fig. 8~~), and~~). However, in the estuarine section, although nitrate concentration was not related to D/L AAs ~~but~~, it ~~indeed~~ was related to GABA% ~~in the estuarine section~~ (Fig. 8b). This indicates that fluvial nitrate in the fresh water section was not derived from remineralization of fluvial organic matter in the river channel, but more likely from other sources (e.g., leaching of soil). In the estuarine section, ~~there may be~~ some DON transformation may have occurred (Jiang et al., 2019), ~~while the~~although leaching from ~~soil process still~~soils cannot be ~~eliminated~~ruled out (Fig. 8). For the particulate phase, no ~~relation can be found~~relationship between nitrate and particulate OM composition was detected (figure not shown).

The atomic DOC/DON ratio in the Rajang averaged 50 in the river part, and increased to 140 (mean value) in the estuary part (Fig. 7). Although the DOC/DON ratio was much higher ~~when compared to~~than in other tropical peatland river waters (around 10; Sjögersten et al., 2011), the ratio ~~is~~was comparable ~~with~~to that in other peatland-draining rivers in Sarawak like the Lupar, Saruba and Maludan rivers (Müller et al., 2015; Müller et al., 2016), which all enter the South China sea. The ratio is also within the reported C/N ratio of peatland and leaves (Müller et al., 2016). For the Amazon ~~river~~River, the DOC ~~versus~~to total nitrogen ratio ranges from 27 to 52 (Hedges et al., 1994)~~.~~

~~Given their reported total nitrogen~~ and, given that this ratio includes inorganic nitrogen, the DOC/DON ratio for the Amazon ~~river~~River would be even higher. Under the background of such high C/N ratios (e.g., 50), transformation of DON to DIN in the estuary further enhanced the high DOC/DON ratio (to 140), and hence a deficiency in terrestrial organic nitrogen output is expected~~.~~ for the Rajang River. We noted that dissolved inorganic nitrogen ~~for~~concentrations in the Rajang ~~is~~were on the order of 10 μM, comparable to DON (Jiang et al., 2019). Terrestrial nitrogen output is an important source for coastal primary production (Jiang et al., 2019), but peatland-impacted rivers may have relatively lower nitrogen input to the South China Sea when compared with their very high river basin DOC yields (Baum et al., 2007). On one hand, logging and secondary growth has been found to play a negative role in the nitrogen output efficiency of forest soils (Davidson et al., 2007). On the other hand, disturbed tropical peatlands could release more DOC in comparison to an undisturbed site (Moore et al., 2013) while the DOC/DON ratio may also decrease along with disturbance of peatland (Kalbitz and Geyer, 2002). Given that secondary growth in the river basin and anthropogenic disturbance of peatland (e.g., drainage and conversion for oil palm) are both common (Hooijer et al., 2015), changes of DOC/DON ratios in the Rajang are complex and further assessment is needed ~~in the future~~.

5. Summary and Conclusion

In August 2016 in the Rajang, we observed that dissolved OM composition (as D/L Glx ratio) was conservatively diluted along with increasing DOC $\delta^{13}C$, indicating that the sources of dissolved OM have a very conservative impact on the OM composition. When D/L Glx ~~ratio was~~ratios were plotted against salinity ~~(as is usually done for an estuarine OM behavior check in many studies),~~

~~such~~, this linear conservative dilution pattern disappeared (Figs. 4a~~&~~ & 5a). This implies that the total addition of DOC in the estuary (peatland/mangrove) had an impact on dissolved OM composition, adding more bio-degraded OM, and resulting in data above the theoretical dilution line (Figs. 4a~~&~~ & 5a). For particulate OM, though the data was variable, the overall decreasing GABA% or D/L ratio ~~along~~ with increasing salinity was much clearer relative to that of dissolved OM (Figs. 4b~~&~~ & 5b). Particulate D/L Glx ratio in the estuary was usually lower ~~when compared with that~~than in the fresh water section (Figs. 6b~~&~~ & c), whereas for dissolved OM, the majority of the samples in the estuary had a D/L Glx ratio similar to ~~that in~~of the fresh water section (Fig. 6a). The difference in OM composition between fresh water and estuarine section suggests that dissolved OM became more degraded while particulate OM became less degraded in the estuary.

The Rajang is characterized by DOC/DON ratios of 50 in the fresh water section, and the further loss of DON in the estuary increased the ratio to 140. Peatland draining and logging/secondary growth are reported to have conflicting impacts on carbon and nitrogen cycling (Davidson et al., 2007; Moore et al., 2013), which may increase fluvial DOC and limit basin nitrogen output, resulting in even larger DOC/DON ratios. Mismatch in carbon and nitrogen loss from tropical rivers due to anthropogenic activities plays a role in material ~~cycle~~cycling in both ~~land~~terrestrial and marine systems, enhancing the role of tropical ~~river~~rivers as ~~a~~ direct sources of carbon ~~source~~ to atmosphere ~~while for~~; the effect of changes in nitrogen ~~change~~output and its ~~further~~ feedback on the carbon cycle needs further monitoring and assessment.

~~At last~~Finally, this work is based on a dry season investigation (August). Though the seasonality for Rajang OM may be moderate (Martin et al., 2018), for biomarkers like amino acids enantiomers further investigation in the wet season is needed.

Acknowledgements

We thank the captain and crew of the boat, ~~as well as~~and other colleagues on board for assistance during the field work. We thank colleagues and students ~~in~~at both Swinburne University of Technology (Sarawak Campus) and ~~in~~the State Key Lab of Estuarine and Coastal Research/East China Normal University~~.~~ for their help in field and/or lab work. We thank Aazani Mujahid ~~in~~at University of Malaysia Sarawak for her help and hospitality during our stay in Malaysia. This work is funded by the National Key Research and Development Program of China (2018YFD0900702), MOHE FRGS 15 Grant (FRGS/1/2015/WAB08/SWIN/02/1) in Malaysia, ARC Linkage Grant LP150100519 in Australia, a SKLEC Open Research Fund (SKLEC-KF201610) and '111' project in SKLEC/ECNU from the Ministry of Education of China and State Administration of Foreign Experts ~~Affaires~~Affairs of China.

References

Amon, R. M. W., Fitznar, H. P., and Benner, R.: Linkages among the bioreactivity, chemical composition, and diagenetic state of marine dissolved organic matter, Limnology and Oceanography, 46, 287-297, 2001.

Baum, A., Rixen, T., and Samiaji, J.: Relevance of peat draining rivers in central Sumatra for the riverine input of dissolved organic carbon into the ocean, Estuarine, Coastal and Shelf Science, 73, 563-570, 2007.

Bianchi, T. S.: The role of terrestrially derived organic carbon in the coastal ocean: A changing paradigm and the priming effect, Proceedings of the National Academy of Sciences, 108, 19473-19481, 2011.

Bianchi, T. S. and Bauer, J. E.: Particulate Organic Carbon Cycling and Transformation. In: Treatise on Estuarine and Coastal Science, Editors-in-Chief: Eric, W. and Donald, M. (Eds.), Academic Press, Waltham, 2011.

Cifuentes, L. A., Coffin, R. B., Solorzano, L., Cardenas, W., Espinoza, J., and Twilley, R. R.: Isotopic and Elemental Variations of Carbon and Nitrogen in a Mangrove Estuary Estuarine Coastal and Shelf Science, 43, 781-800, 1996.

Cloern, J. E., Foster, S. Q., and Kleckner, A. E.: Phytoplankton primary production in the world's estuarine-coastal ecosystems, Biogeosciences, 11, 2477-2501, 2014.

Dauwe, B. and Middelburg, J. J.: Amino acids and hexosamines as indicators of organic matter degradation state in North Sea sediments, Limnology and Oceanography, 43, 782-798, 1998.

Davidson, E. A., de Carvalho, C. J. R., Figueira, A. M., Ishida, F. Y., Ometto, J. P. H. B., Nardoto, G. B., Saba, R. T., Hayashi, S. N., Leal, E. C., Vieira, I. C. G., and Martinelli, L. A.: Recuperation of nitrogen cycling in Amazonian forests following agricultural abandonment, Nature, 447, 995-998, 2007.

Davis, J., Kaiser, K., and Benner, R.: Amino acid and amino sugar yields and compositions as indicators of dissolved organic matter diagenesis, Organic Geochemistry, 40, 343-352, 2009.

Dittmar, T., Fitznar, H. P., and Kattner, G.: Origin and biogeochemical cycling of organic nitrogen in the eastern Arctic Ocean as evident from D- and L-amino acids, Geochimica et Cosmochimica Acta, 65, 4103-4114, 2001a.

Dittmar, T., Lara, R. J., and Kattner, G.: River or mangrove? Tracing major organic matter sources in tropical Brazilian coastal waters, Marine Chemistry, 73, 253-271, 2001b.

Fitznar, H. P., Lobbes, J. M., and Kattner, G.: Determination of enantiomeric amino acids with high-performance liquid chromatography and pre-column derivatisation with o-phthaldialdehyde and N-isobutyrylcysteine in seawater and fossil samples (mollusks), Journal of Chromatography A, 832, 123-132, 1999.

Gandois, L., Teisserenc, R., Cobb, A. R., Chieng, H. I., Lim, L. B. L., Kamariah, A. S., Hoyt, A., and Harvey, C. F.: Origin, composition, and transformation of dissolved organic matter in tropical peatlands, Geochimica et Cosmochimica Acta, 137, 35-47, 2014.

Hedges, J. I., Cowie, G. L., Richey, J. E., Quay, P. D., Benner, R., Mike, S., and Forsberg, B. R.: Origins and processing of organic matter in the Amazon River as indicated by carbohydrates and amino acids, Limnology and Oceanography, 39, 743-761, 1994.

Hedges, J. I. and Man, D. C.: The characterization of plant tissues by their lignin oxidation products, Geochimica et Cosmochimica Acta, 43, 1803-1807, 1979.

Hernes, P. J., Robinson, A. C., and Aufdenkampe, A. K.: Fractionation of lignin during leaching and sorption and implications for organic matter “freshness”, Geophysical Research Letters, 34, 2007.

Hooijer, A., Vernimmen, R., Visser, M., and Mawdsley, N.: Flooding projections from elevation and subsidence models for oil palm plantations in the Rajang delta peatlands, Sarawak, Malaysia, Deltares report 1207384, 76 pp., 2015.

Huang, T. H., Chen, C. T. A., Tseng, H. C., Lou, J. Y., Wang, S. L., Yang, L., Kandasamy, S., Gao, X., Wang, J. T., Aldrian, E., Jacinto, G. S., Anshari, G. Z., Sompongchaiyakul, P., and Wang, B. J.: Riverine carbon fluxes to the South China Sea, Journal of Geophysical Research: Biogeosciences, 122, 1239-1259, 2017.

Jennerjahn, T. C., Ittekkot, V., Klöpper, S., Adi, S., Purwo Nugroho, S., Sudiana, N., Yusmal, A., Prihartanto, and Gaye-Haake, B.: Biogeochemistry of a tropical river affected by human activities in its catchment: Brantas River estuary and coastal waters of Madura Strait, Java, Indonesia, Estuarine, Coastal and Shelf Science, 60, 503-514, 2004.

Jiang, S., Müller, M., Jin, J., Wu, Y., Zhu, K., Zhang, G., Mujahid, A., Rixen, T., Muhamad, M. F., Sia, E. S. A., Jang, F. H. A., and Zhang, J.: Dissolved inorganic nitrogen in a tropical estuary at Malaysia: transport and transformation, Biogeosciences Discuss., 2019, 1-27, 2019.

Kaiser, K. and Benner, R.: Biochemical composition and size distribution of organic matter at the Pacific and Atlantic time-series stations, Marine Chemistry, 113, 63-77, 2009.

Kaiser, K. and Benner, R.: Hydrolysis-induced racemization of amino acids, Limnology and Oceanography: Methods, 3, 318-325, 2005.

Kalbitz, K. and Geyer, S.: Different effects of peat degradation on dissolved organic carbon and nitrogen, Organic Geochemistry, 33, 319-326, 2002.

Kimber, R. W. L., Nannipieri, P., and Ceccanti, B.: The degree of racemization of amino acids released by

hydrolysis of humic-protein complexes: Implications for age assessment, Soil Biology and Biochemistry, 22, 181-185, 1990.
Lamade, E., Setiyo, I. E., Girard, S., and Ghashghaie, J.: Changes in 13C/12C of oil palm leaves to understand carbon use during their passage from heterotrophy to autotrophy, Rapid Communications in Mass Spectrometry, 23, 2586-2596, 2009.
Lamb, A. L., Wilson, G. P., and Leng, M. J.: A review of coastal palaeoclimate and relative sea-level reconstructions using δ13C and C/N ratios in organic material, Earth-Science Reviews, 75, 29-57, 2006.
Martin, P., Cherukuru, N., Tan, A. S. Y., Sanwlani, N., Mujahid, A., and Müller, M.: Distribution and cycling of terrigenous dissolved organic carbon in peatland-draining rivers and coastal waters of Sarawak, Borneo, Biogeosciences, 15, 6847-6865, 2018.
Mayorga, E., Aufdenkampe, A. K., Masiello, C. A., Krusche, A. V., Hedges, J. I., Quay, P. D., Richey, J. E., and Brown, T. A.: Young organic matter as a source of carbon dioxide outgassing from Amazonian rivers, Nature, 436, 538-541, 2005.
Moore, S., Evans, C. D., Page, S. E., Garnett, M. H., Jones, T. G., Freeman, C., Hooijer, A., Wiltshire, A. J., Limin, S. H., and Gauci, V.: Deep instability of deforested tropical peatlands revealed by fluvial organic carbon fluxes, Nature, 493, 660, 2013.
Müller-Dum, D., Warneke, T., Rixen, T., Müller, M., Baum, A., Christodoulou, A., Oakes, J., Eyre, B. D., and Notholt, J.: Impact of peatlands on carbon dioxide (CO2) emissions from the Rajang River and Estuary, Malaysia, Biogeosciences, 16, 17-32, 2019.
Müller, D., Warneke, T., Rixen, T., Müller, M., Jamahari, S., Denis, N., Mujahid, A., and Notholt, J.: Lateral carbon fluxes and CO2 outgassing from a tropical peat-draining river, Biogeosciences, 12, 5967-5979, 2015.
Müller, D., Warneke, T., Rixen, T., Müller, M., Mujahid, A., Bange, H. W., and Notholt, J.: Fate of terrestrial organic carbon and associated CO2 and CO emissions from two Southeast Asian estuaries, Biogeosciences, 13, 691-705, 2016.
Raymond, P. A. and Bauer, J. E.: Use of 14C and 13C natural abundances for evaluating riverine, estuarine, and coastal DOC and POC sources and cycling: a review and synthesis, Organic Geochemistry, 32, 469-485, 2001.
Schleifer, K. H. and Kandler, O.: Peptidoglycan types of bacterial cell walls and their taxonomic implications, Bacteriological Reviews, 36, 407-477, 1972.
Schroeder, R. A. and Bada, J. L.: A review of the geochemical applications of the amino acid racemization reaction, Earth-Science Reviews, 12, 347-391, 1976.
Sjögersten, S., Cheesman, A. W., Lopez, O., and Turner, B. L.: Biogeochemical processes along a nutrient gradient in a tropical ombrotrophic peatland, Biogeochemistry, 104, 147-163, 2011.
Vollmer, W., Blanot, D., and de Pedro, M.: Peptidoglycan structure and architecture, FEMS Microbiology Review, 32, 149-167, 2008.
Wu, Y., Zhu, K., Zhang, J., Müller, M., Jiang, S., Mujahid, A., Muhamad, M. F., and Sia, E. S. A.: Distribution and degradation of terrestrial organic matter in the sediments of peat-draining rivers, Sarawak, Malaysian Borneo, Biogeosciences Discuss., 2019, 1-37, 2019.
Zhang, C. L., Dang, H. Y., Azam, F., Benner, R., Legendre, L., Passow, U., Polimene, L., Robinson, C., Suttle, C. A., and Jiao, N. Z.: Evolving paradigms in biological carbon cycling in the ocean, National Science Review, 5, 481-499, 2018.
Zhu, Z. Y., Wu, Y., Zhang, J., Dittmar, T., Li, Y., Shao, L., and Ji, Q.: Can primary production contribute non-labile organic matter in the sea: Amino acid enantiomers along the coast south of the Changjiang

554 Estuary in May, Journal of Marine Systems, 129, 343-349, 2014.
555 Zhu, Z. Y., Zhang, J., Wu, Y., and Lin, J.: Bulk particulate organic carbon in the East China Sea: Tidal
556 influence and bottom transport, Progress in Oceanography, 69, 37-60, 2006.
557
558

559 Table 1. Measured amino acids (the L- and D- enantiomers are not listed) and all abbreviations in
560 this study. Note that glycine has no enantiomer.

name	abbreviations
organic matter	OM
dissolved organic carbon	DOC
dissolved organic nitrogen	DON
total suspended matter	TSM
amino acid	AA
total hydrolysable dissolved amino acids	TDAA
total hydrolysable particulate amino acids	TPAA
Alanine	Ala
Arginine	Arg
Asparagine	Asx
Aspartic acid	
Glutamine	Glx
Glutamic acid	
Glycine	Gly
Isoleucine	Ile
Leucine	Leu
Lysine	Lys
Methionine	Met
Phenylalanine	Phe
Serine	Ser
Threonine	Thr
Tryptophan	Trp
Tyrosine	Tyr
Valine	Val
γ - aminobutyric acid	GABA

561
562

Table 2. TSM, DOC, POC and stable carbon isotopes in the freshwater and estuary of the Rajang (mean (min-max)).

	unit	Fresh water	Estuary
TSM	mg/L	61 (22 - 126)	73 (25 - 161)
DOC	µM	337 (217 - 658)	345 (214 - 587)
DOC $\delta^{13}C$	‰	–26.7 (–27.7 - –25.0)	–26.1 (–28.7 - –20.1)
POC	µM	86 (46 - 125)	64 (22 - 153)
	%	1.9 (1.2 - 2.5)	1.0 (0.6 - 1.9)
POC $\delta^{13}C$	‰	–30.1 (–31.1 - –29.4)	–26.7 (–30.1 - –23.8)

Table 3 ~~The~~ Rajang AAs ~~result~~ (mean (min-max)) in August 2016 (*~~total~~Total D/TDAA ~~means~~= total D form AA versus TDAA~~, the same for total~~. Total D/TPAA = total D form AA versus TPAA)

		unit	Fresh water	Estuary
dissolved	TDAA	nM	317 (131 - 486)	523 (212 - 2320)
	TDAA carbon yield	%	0.40 (0.08 - 0.65)	0.38 (0.29 - 0.53)
	TDAA nitrogen yield	%	4.8 (1.3 - 15)	11 (5.4 - 18)
	GABA	%	2.0 (1.3 - 4.1)	1.3 (0.15 - 1.9)
	total D/total TDAA*	%	12 (8 - 15)	12 (3 - 14)
	D/L Glx		0.35 (0.16 - 0.57)	0.32 (0.07 - 0.42)
	D/L Asx		0.34 (0.23 - 0.48)	0.34 (0.08 - 0.42)
particulate	TPAA	µM	2.5 (1.4 - 3.6)	2.0 (1.1 - 3.7)
	TPAA carbon yield	%	14 (9.5 - 19)	17 (11 - 24)
	TPAA nitrogen yield	%	66 (36 - 82)	62 (30 - 100)
	GABA%	%	0.7 (0.6 - 0.9)	0.4 (0.2 - 0.8)
	total D/total TPAA*	%	4.4 (3.6 - 5.2)	3.3 (2.4 - 5.0)
	D/L Glx		0.09 (0.08 - 0.10)	0.06 (0.04 - 0.08)
	D/L Asx		0.04 (0.03 - 0.05)	0.05 (0.03 - 0.11)

Figure caption

Figure 1. Study area and sampling stations. a) Location of Sarawak, Malaysia; and b) the Rajang with its estuary/river mouth ~~background~~ shown. Samples upstream of S5 ~~showed~~had 0 salinity ~~while~~and downstream of S5 ~~showed~~had salinity >0. Hence~~ here,~~ from S5 to S10 ~~is~~was regarded as the fresh water section (red triangles), and downstream of S5 ~~is~~was regarded as the estuarine section (blue triangles). Note that salinity of samples at S15, S17, S18, S19 was also 0 during our sampling.

Figure 2. Distribution ~~pattern~~patterns of (a) TSM, (b) DOC and (c) POC along with salinity in the Rajang. The fresh water ~~dot stands for~~data point represents all samples with ~~S~~salinity = 0 and the error bar corresponds to the standard deviation. The marine ~~dot is~~data point represents S1.

Figure 3. Distribution ~~pattern~~patterns of (a) DOC $\delta^{13}C$ and (b) POC $\delta^{13}C$ along with conductivity/salinity in the Rajang. The legend indicates the branches that the samples were collected from and the marine ~~corresponds~~data points correspond to ~~S1~~ station S1.

Figure 4. The GABA% distribution pattern from fresh water to the estuary in the Rajang: a) dissolved and b) particulate. Note the different x-axis scales between plot a and b. The dashed line indicates the linear mixing line between fresh and marine endmembers. ~~For the~~The fresh water endmember (brown triangle~~), it is~~) was calculated as the ~~means~~mean of all fresh water samples (~~S~~salinity = 0), and the marine endmember (purple diamond) ~~is~~was calculated as the ~~means~~mean of all offshore samples with salinity >30. The error bar indicates the standard deviation.

~~Figure 5. Same as figure 4, but for D/L Glx.~~

Figure 5. The D/L Glx distribution pattern from fresh water to the estuary in the Rajang: a) dissolved and b) particulate. Note the different x-axis scales between plot a and b. The dashed line indicates the linear mixing line between fresh and marine endmembers. The fresh water endmember (brown triangle) was calculated as the mean of all fresh water samples (salinity = 0), and the marine endmember (purple diamond) was calculated as the mean of all offshore samples with salinity >30. The error bar indicates the standard deviation.

Figure 6. D/L ratio of AAs (as Glx) plotted against a) DOC $\delta^{13}C$ b) POC $\delta^{13}C$, and c) PN $\delta^{15}N$.

Figure 7. DOC/DON ratio distribution pattern along with salinity in the Rajang. For fresh water and estuary, the mean DOC/DON value was 50 and 140, respectively. DON ~~is~~concentrations are taken from Jiang et al., (2019~~)~~).

Figure 8. Dissolved OM composition (a: D/L Glx, b: GABA%) and its ~~relation~~relationship with nitrate~~.~~ concentration. Nitrate ~~is derived~~concentrations are taken from Jiang et al., (2019).

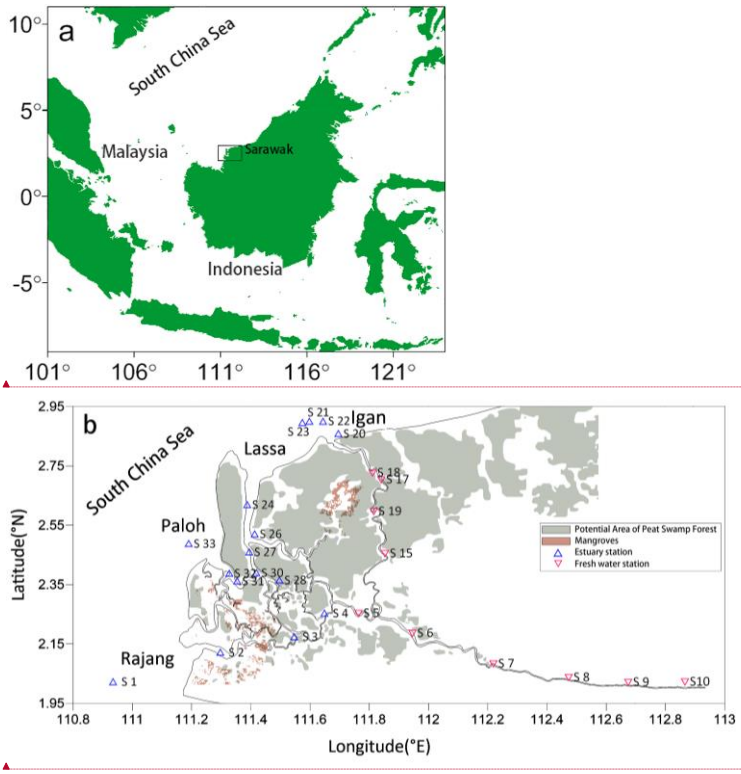

Figure 1.

带格式的：英语(澳大利亚)

带格式的：英语(澳大利亚)

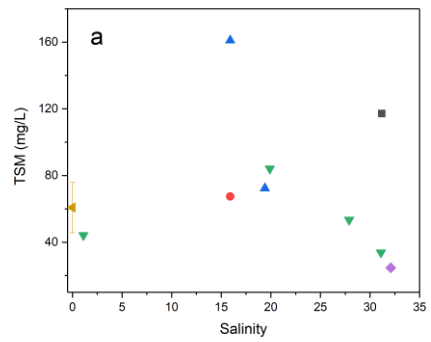

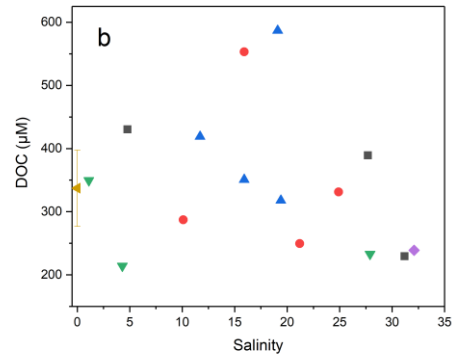

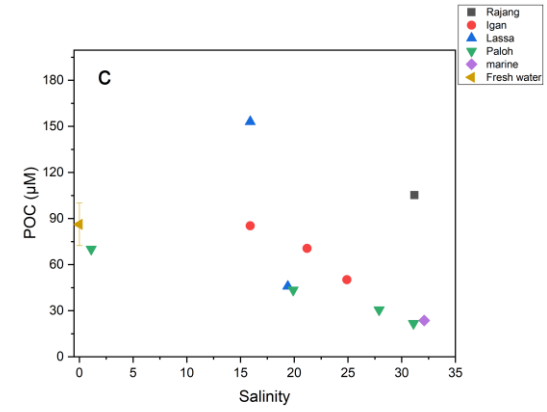

Figure 2.

带格式的：英语(澳大利亚)

带格式的：英语(澳大利亚)

带格式的：英语(澳大利亚)

622

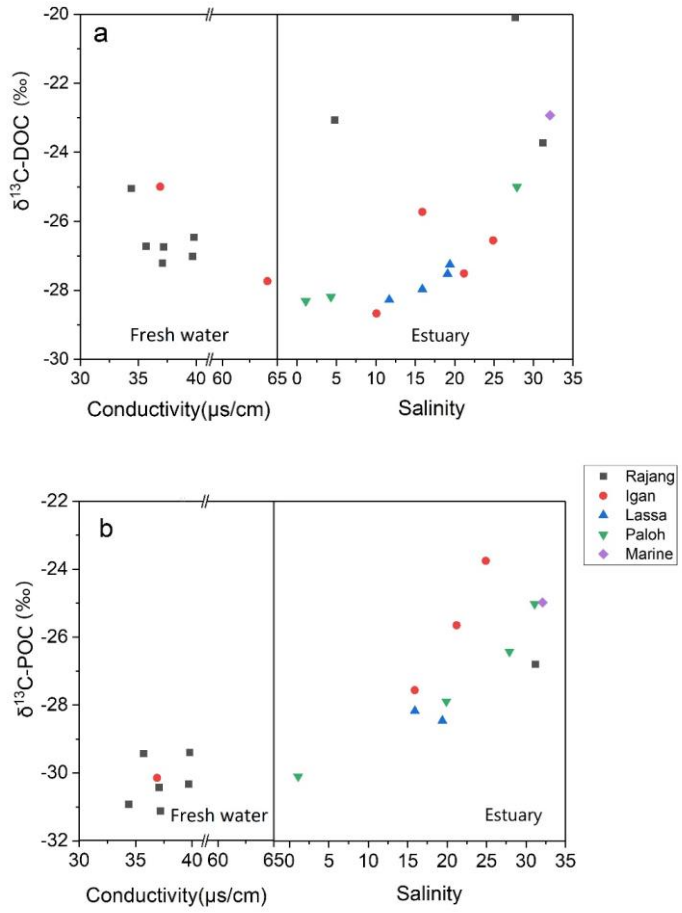

623 Figure 3.

624

625

626

带格式的：英语(澳大利亚)

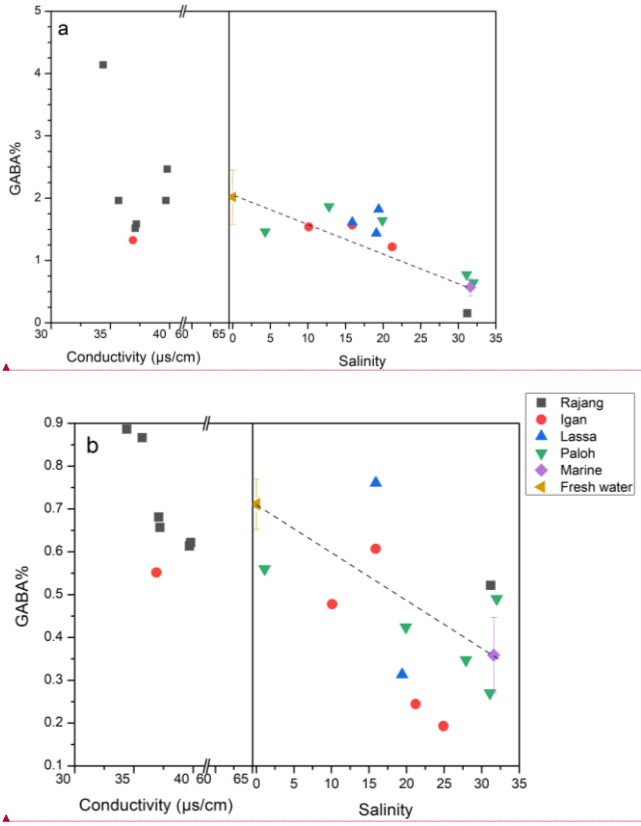

Figure 4.

带格式的：英语(澳大利亚)

带格式的：英语(澳大利亚)

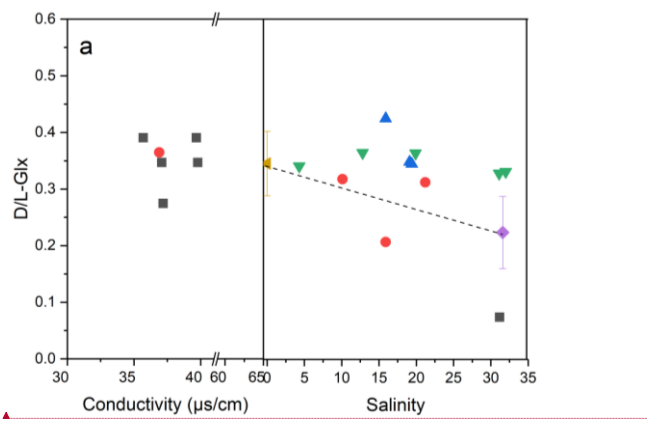

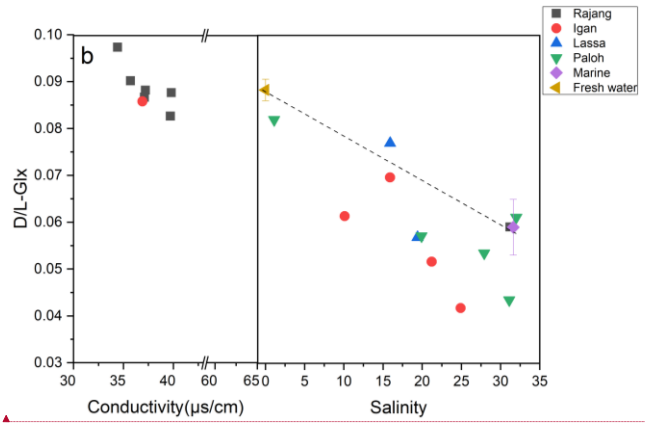

Figure 5.

带格式的：英语(澳大利亚)

带格式的：英语(澳大利亚)

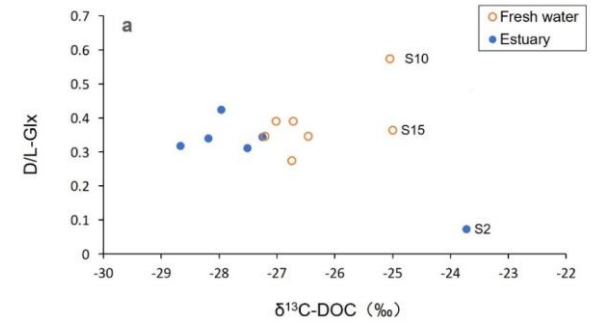
a
Fresh water
Estuary
S10
S15
S2
D/L-Glx
δ13C-DOC（‰）

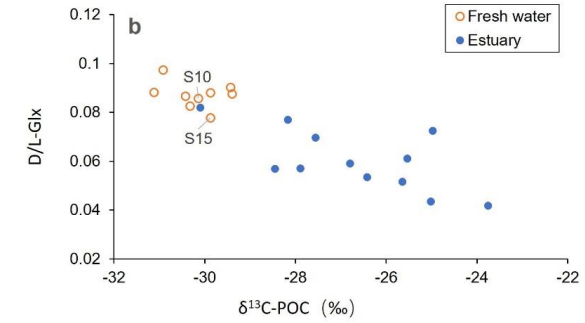
b
Fresh water
Estuary
S10
S15
D/L-Glx
δ13C-POC（‰）

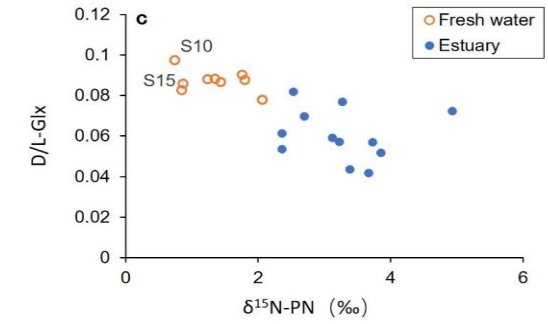
c
Fresh water
Estuary
S10
S15
D/L-Glx
δ15N-PN（‰）

Figure 6.

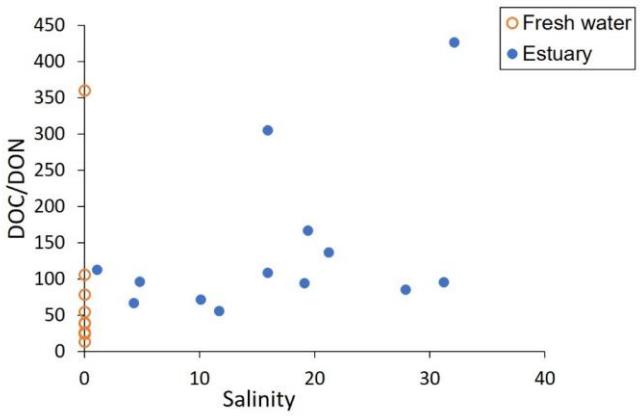

Figure 7.

带格式的：英语(澳大利亚)

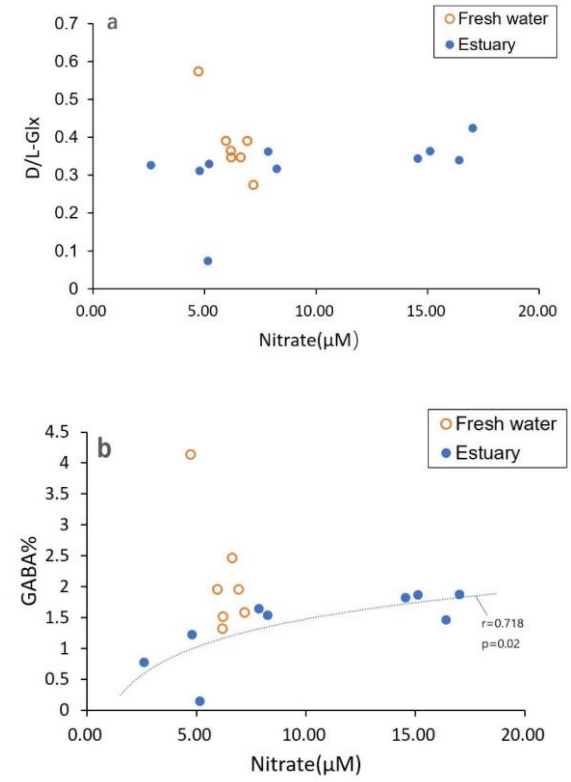

Figure 8.

带格式的：英语(澳大利亚)

带格式的：英语(澳大利亚)